Visualizing coherent phonon propagation in the 100 GHz range: A broadband picosecond acoustics approach

Emanuele Pontecorvo,[1] Michele Ortolani,[2] Dario Polli,[3] Marco Ferretti,[1] Giancarlo Ruocco,[1,4] Giulio Cerullo,[3] and Tullio Scopigno[1,4,a)]
[1]*Dipartimento di Fisica, Universitá di Roma "Sapienza", I-00185 Roma, Italy*
[2]*IFN-CNR, Via Cineto Romano 42, 00156 Rome, Italy*
[3]*IFN-CNR, Dipartimento di Fisica, Politecnico di Milano, P.zza L. da Vinci 32, 20133 Milano, Italy*
[4]*IPCF-CNR, Sezione Sapienza, c/o Dipartimento di Fisica, Universitá di Roma "La Sapienza", I-00185 Roma, Italy*

(Received 17 September 2010; accepted 23 September 2010; published online 3 January 2011)

Building on a 1 kHz amplified Ti:sapphire laser source, we developed a novel pump-probe setup for broadband picosecond acoustics using a white-light continuum probe coupled to an optical multichannel analyzer. The system allows one to access, in a single measurement, acoustic parameters such as sound velocity and attenuation all over the bandwidth of the acoustic wave-packet launched by the pump pulse. We use the setup to measure the sound attenuation in fused silica and observe a dynamic crossover occurring at ≈170 GHz. © *2011 American Institute of Physics*. [doi:10.1063/1.3532961]

The behavior of high-frequency acoustic excitations in disordered materials is one of the most provocative and less understood aspects of glass science, and is intimately related to the origin of the low temperature thermodynamical anomalies in amorphous materials.[1] The frequency (ν) dependence of sound damping (Γ), in particular, is the result of the interplay of several physical mechanisms crucial for many theoretical models.[2–6] A benchmark to study sound damping in disordered materials is vitreous silica, the prototypical covalently bonded glass former. In this system anharmonicity of the interparticle interactions rules a low frequency region (acoustic excitations wavelengths $\lambda_a > 100$ nm) where the sound attenuation follows an ν^2 law in agreement with the predictions of the Akhiezer mechanism.[3] Of great interest is the opposite limit, where the wavelength is comparable with the interparticle distance, a region which became accessible thanks to the development of inelastic x-ray scattering technique.[7] Experiments indicate also here a ν^2 dependence of the sound damping, but with a different (higher) coefficient. Hence, one legitimately expects a crossover between these two behaviors, which should occur at acoustic wavelengths between 100 and 10 nm (corresponding to frequencies between 60 and 600 GHz). This crossover is expected to be ruled by an ν^4 behavior, which is typical of Rayleigh scattering regime when acoustic waves are diffused by uncorrelated pointlike defects.[2,8] This frequency region, unfortunately, is hardly accessible by spectroscopic techniques in the frequency domain.

Interferometric picosecond acoustics (PA) is a powerful time-domain approach for the study of sound attenuation in amorphous materials. PA is a pump-probe technique in which an ultrashort optical pump pulse is partially absorbed by a thin metallic transducing layer, deposited onto the surface of the sample, and launches by "instantaneous" thermal expansion a longitudinal acoustic wave-packet with a characteristic spectrum extending in the 40–400 GHz region.[9] The acoustic pulse then travels inside the sample and its motion is monitored by a delayed optical probe pulse with wavelength λ_{pr}. The probe pulse is reflected by the strain wave through a (stimulated) Brillouin scattering process, i.e., interacting with a single phonon frequency

$$\nu = \frac{cq}{2\pi} = \frac{2nc}{\lambda_{pr}} \cos\,\theta, \tag{1}$$

where c is the sound velocity, q the acoustic wave vector, $n(\lambda_{pr})$ the refractive index of the medium and θ the scattering angle. The Brillouin scattered intensity interferes with the portion of probe beam reflected by the fixed metallic layer, leading to time-dependent oscillations with a periodicity T set by the Bragg condition: $T = \frac{\lambda_{pr}}{2cn\,\cos\,\theta}$, i.e., corresponding to the period of the phase-matched acoustic phonon. The periodicity and damping of such oscillations then gives direct access to acoustic parameters such as sound velocity and attenuation. Traditionally PA experiments are implemented using Ti:sapphire oscillators with ≈100 MHz repetition rate, providing both ≈800 nm pump and frequency doubled ≈400 nm probe pulses, with a duration of ≈100 fs. These high repetition rate systems, combined with high-frequency modulation and lock-in amplification, provide a very good signal-to-noise ratio, with differential reflectivity ($\Delta R/R$) down to 10^{-7}, but only a limited wavelength range in detection; in addition, only one probe wavelength at a time is recorded, calling for a time-consuming, less efficient procedure in order to measure the frequency dependence of sound parameters.

In this letter, we report on a broadband version of interferometric PA, which allows accessing in a single measurement a nearly octave-spanning range of the acoustic frequency wave-packet with unprecedented sampling efficiency. Our system is based on a 1 kHz amplified Ti:sapphire laser and uses a white-light continuum (WLC) probe in combination with an optical multichannel analyzer (OMA). We have used our setup to study samples of thermally grown silica, following the phase-matching layout proposed in Refs. 10 and 11, and were able to observe a crossover in sound at-

a)Author to whom correspondence should be addressed: tullio.scopigno@roma1.infn.it.

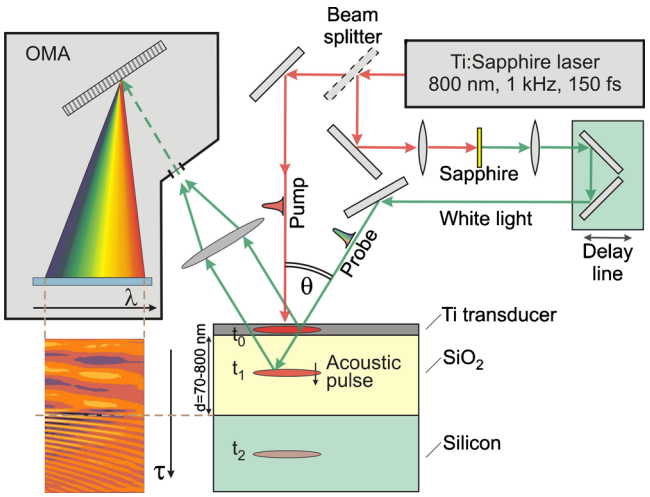

FIG. 1. (Color online) Schematic layout of the broadband picosecond acoustics setup that we used to measure sound attenuation in vitreous silica.

tenuation around 170 GHz. A schematic layout of the broadband PA setup is shown in Fig. 1. It is based on a regeneratively amplified Ti:sapphire laser (Clark-MXR, Model CPA-1) producing 150 fs, 500−μJ pulses at 800 nm wavelength and 1 kHz repetition rate. A portion of this beam (the pump, with energy up to 5 μJ) is loosely focused on the sample. Another fraction of the pulse is focused in a 2-mm-thick sapphire plate to generate a broadband single-filament WLC which, after passing through a delay line, acts as a probe. The visible portion of the WLC, extending from 430 to 760 nm, is also focused on the sample and the reflected light is dispersed on an OMA equipped with fast electronics, allowing single-shot recording of the probe spectrum at the full 1 kHz repetition rate.[12] Our setup achieves for each channel sensitivity down to $\Delta R/R \approx 10^{-5}$, allowing continuous monitoring of the sound parameters (speed and attenuation) over a broad range of frequencies in a single measurement.

The technique has been applied to a set of pure silica (v-SiO_2) samples of different thicknesses, obtained starting from a 0.8-μm-thick layer grown on the polished surface of a [111] silicon wafer by oxidation in N_2/H_2O atmosphere in a furnace at 950 °C. The wafer was then cut into several portions, each of them exposed for a different time to an HF-based etching solution to uniformly decrease the SiO_2 layer thickness in the range 70–800 nm. The resulting thickness values for the different wafer portions were determined by spectroscopic ellipsometry. In this way we obtained a series of samples with identical microscopic mechanical properties, but different SiO_2 layer thicknesses. Finally, a 10-nm-thick Ti transducer layer was deposited on all samples in a single evaporation process, to ensure identical acoustic wave-packet properties for the whole series. We employed Ti as transducer because of its resistance to the high energy of our amplified pulses. The metal/SiO_2/Si structure, as demonstrated in Refs. 13–15, allows extending upwards the accessible acoustic frequency range since, when entering the Si substrate, the phase-matched acoustic frequency becomes approximately five times larger, due to the larger value of sound speed ($c^{(Si)}=9.36$ km/s) and refractive index ($n^{(Si)}_{max}=6.8$ at $\lambda_{pr}\approx 370$ nm) compared to silica ($c^{(SiO_2)}=5.95$ km/s, $n^{(SiO_2)}\simeq 1.5$).

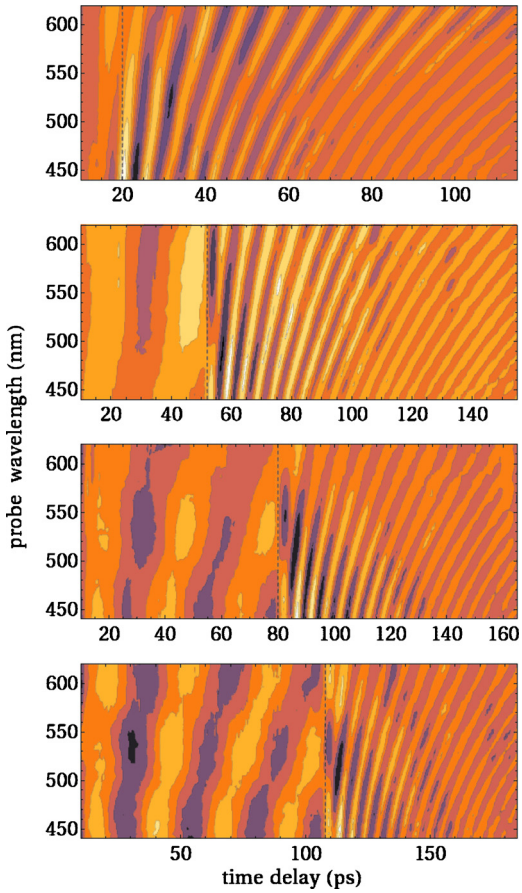

FIG. 2. (Color online) Oscillatory component of the $\Delta R/R$ map for d=70, 313, 483, 642 nm (top to bottom) SiO_2 films on a Si substrate.

Figure 2 shows the measured maps of the oscillatory component of the normalized $\Delta R/R$ as a function of probe wavelength and delay obtained by this technique on four samples of different thicknesses. An exponential background, due to slowly varying, transient changes of the refractive index in the transducer, has been preliminarily removed from the entire matrix.[16,17] One can immediately recognize that each probe wavelength, λ_{pr}, is phase-matched according to Eq. (1) with a well defined acoustic frequency, ν, which changes when the acoustic wave-packet leaves silica entering in silicon. Figure 3 shows a typical $\Delta R/R$ time trace (panel A) for $d=483$ nm sample thickness and probe wavelength $\lambda_1=464$ nm, corresponding to an acoustic frequency $\nu=183$ GHz. For a given λ_{pr} the amplitude of the oscillation in silicon at the Si/SiO_2 interface, A_{Si}, mainly depends on: (i) how much the corresponding Fourier component of the acoustic wave-packet has been attenuated while traveling through the SiO_2 film; (ii) how "efficiently" the acoustic wave-packet reflects the probe pulse in silicon: the oscillation amplitude increases indeed with decreasing probe wavelenghts due to the enhancement of the Si acousto-optic coupling coefficients upon approaching the direct band gap value at 364 nm. One can get rid of this second dependence by repeating the measurements for a set of samples with different SiO_2 film thicknesses d (Ref. 14): in panel B we report $A_{Si}(d)$ values—for the same $\lambda=464$ nm—weighted by the intensity in the $SiO_2(A_{SiO_2})$ (as obtained from the amplitudes of the sinusoidal fits), to account for possible changes of the overall signal intensity when switching from one sample to another of different thickness. A clear expo-

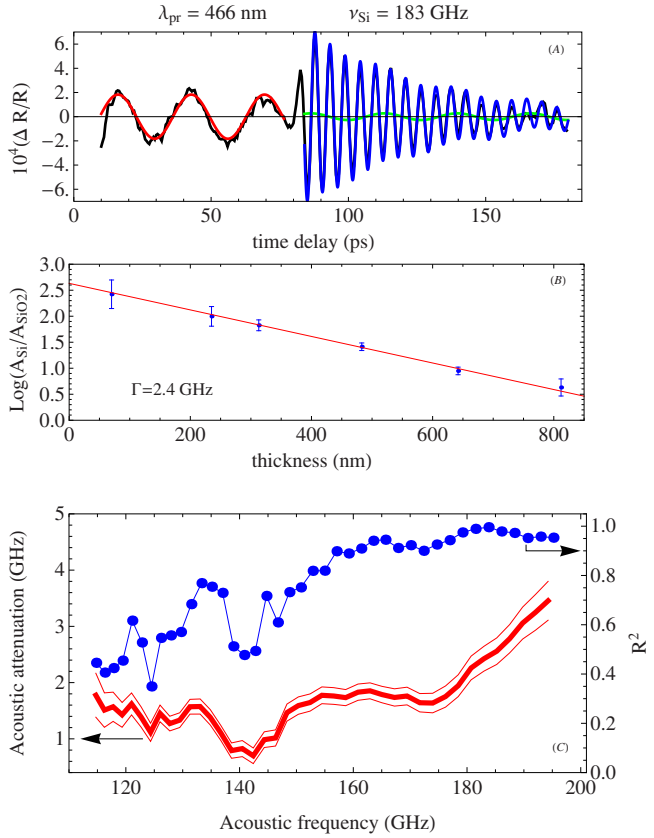

FIG. 3. (Color online) Panels A: $\Delta R/R$ trace for a d=483 nm SiO_2 film and 464 nm probe wavelength. The longer wavelength sinusoidal line (red) is the best fit in the SiO_2 region, partially back-reflected at the Si interface after ≈80 ps (green), while the shorter wavelength damped sinusoidal line is the best fit in the Si region. Panels B: Reflected amplitudes for different thicknesses d, continuous red line is the best exponential fit. Panel C: thick (red) line is the attenuation coefficient with 95% confidence bands, while (blue) circles with guideline are the regression coefficient of the exponential fits.

nential decay $\frac{A_{Si}(d)}{A_{SiO_2}} \propto e^{-d/l}$, with l the mean free path (MFP) of acoustic waves, is detected. The quality of the exponential fit varies significantly with the acoustic frequency. Below ν=150 GHz deviations are observed, as shown by the regression coefficient, R^2, reported in panel C. The analysis of the interference pattern in the present experimental configuration is indeed intrinsically more complex than a simple metal/SiO_2 layout. One has to consider also the reflection from the fixed SiO_2/Si interface, which modulates the exponential thickness-dependent behavior of the intensity expected for a simple interference between the pulses reflected at the (fixed) metal layer and those backscattered by the (moving) strain wave.[18] This effect, which might be responsible for the relatively low and scattered R^2 values below 150 GHz, can be in principle modeled but, as a matter of fact, the corrections critically depend on several experimental parameters.[18,19] Finally, we determined sound attenuation Γ from the MFP via the expression $\Gamma=\frac{c}{2\pi l}$, obtaining the frequency dependence of the sound attenuation reported in Fig. 3(c). The present broadband PA data clearly indicate a crossover at $\nu \approx 175$ GHz.

In conclusion, using a 1 kHz Ti:sapphire, we demonstrated a broadband approach to time domain PA experiments to study vibrational properties of few microns thick (i.e., bulklike) specimens. The use of a broadband WLC probe, together with a fast OMA, allows for the determination, in a single measurement, of acoustic waves frequency and attenuation in a broad range around ≈100 GHz, greatly improving measurement efficiency and accuracy. By a suitable choice of the sample substrate, one can in fact cover the whole bandwidth of the acoustic wave-packet launched by the pump pulse. Applying this technique to the case of v-SiO_2, we determined the sound attenuation and found the existence of a "high-frequency" Rayleigh regime with an onset at ≈170 GHz.

E.P. and T.S. acknowledge support from the European Research Council under the European Community Seventh Framework Program (FP7/2008-2013)/ERC IDEAS Grant Agreement No. 207916.

[1]R. C. Zeller and R. O. Pohl, Phys. Rev. B **4**, 2029 (1971).
[2]J. W. S. Rayleigh, *The Theory of Sound* (Mc Millan, London, 1986).
[3]A. Akhiezer, J. Phys. (USSR) **1**, 277 (1939).
[4]U. Buchenau, Y. M. Galperin, V. L. Gurevich, D. A. Parshin, M. A. Ramos, and H. R. Schober, Phys. Rev. B **46**, 2798 (1992).
[5]W. Schirmacher, G. Diezemann, and C. Ganter, Phys. Rev. Lett. **81**, 136 (1998).
[6]J. Fabian and P. B. Allen, Phys. Rev. Lett. **82**, 1478 (1999).
[7]F. Sette, M. Krisch, C. Masciovecchio, G. Ruocco, and G. Monaco, Science **280**, 1550 (1998).
[8]P. G. Klemens, Proc. Phys. Soc., London, Sect. A **68**, 1113 (1955).
[9]C. Thomsen, J. Strait, Z. Vardeny, H. J. Maris, J. Tauc, and J. J. Hauser, Phys. Rev. Lett. **53**, 989 (1984).
[10]A. Devos and R. Côte, Phys. Rev. B **70**, 125208 (2004).
[11]A. Devos, R. Côte, G. Caruyer, and A. Lefèvre, Appl. Phys. Lett. **86**, 211903 (2005).
[12]D. Polli, L. Lüer, and G. Cerullo, Rev. Sci. Instrum. **78**, 103108 (2007).
[13]A. Devos, J.-F. Robillard, R. Côte, and P. Emery, Phys. Rev. B **74**, 064114 (2006).
[14]A. Devos, M. Foret, S. Ayrinhac, P. Emery, and B. Rufflé, Phys. Rev. B **77**, 100201 (2008).
[15]H. Ogi, T. Shagawa, N. Nakamura, M. Hirao, H. Odaka, and N. Kihara, Phys. Rev. B **78**, 134204 (2008).
[16]H. Pedersen, R. Bro, and S. Engelsen, J. Magn. Reson. **157**, 141 (2002).
[17]S. Engelsen and R. Bro, J. Magn. Reson. **163**, 192 (2003).
[18]O. B. Wright, J. Appl. Phys. **71**, 1617 (1992).
[19]O. Matsuda and O. B. Wright, J. Opt. Soc. Am. B **19**, 3028 (2002).